Journal of Chromatography, 254 (1983) 1–14
Elsevier Scientific Publishing Company, Amsterdam — Printed in The Netherlands

CHROM. 15,317

SINGLE-TEMPERATURE DESORPTION FROM POROUS CATALYSTS

R. O. HIDALGO and B. J. McCOY*
Department of Chemical Engineering, University of California, Davis, CA 95616 (U.S.A.)
(Received June 14th, 1982)

SUMMARY

Comparison between continuous-flow stirred tank and column models for single-temperature desorption processes, with and without intraparticle considerations, shows the effect of dispersion, mass transfer, and diffusion phenomena on temporal moment expressions for output concentrations. Substantial differences are found between stirred-tank and column models for beds of porous spherical particles. Elution curves for adsorption sites with different values of the equilibrium coefficient K are constructed from the moments. Bimodal peaks are predicted for a single-temperature desorption if the K values for two different sites are sufficiently different. Commonly used shape indicators are related to the temporal moments.

INTRODUCTION

Desorption methods are important in the study of active sites for adsorption and catalysis on porous solids. The study of thermal desorption processes[1–5] has been restricted principally to systems in which the temperature is varied continuously with time (temperature programmed desorption, TPD). Linear increases in temperature are usually used in experimental measurements and in the theoretical models for the prediction of concentration responses from such systems. Mass transfer and intraparticle diffusion considerations have usually been neglected in the studies, which are based on a continuous-flow stirred tank (CST) model with a steady state simplification. The application of a model with perfect mixing, the CST model, to an experimental configuration which is usually tubular[3] apparently has not been questioned up to now. The quantitative effects of longitudinal dispersion and intraparticle diffusion have not been definitively established.

In the present work such mass transport effects are considered for the CST and column models, and their importance is assessed. Although the analysis is based on a constant (or step increase) temperature desorption, the major qualitative conclusions regarding mixing and mass transfer are expected to apply to temperature programmed desorption processes since the transport parameters are not strong functions of temperature. A method of representing elution concentration profiles in terms of moments by a series expansion in orthogonal functions shows that multi-model elution profiles are a consequence of different values of adsorption equilibrium coef-

0021-9673/83/0000–0000/$03.00

ficients, and not necessarily of temperature programming. Shape indicators, which have been defined and used to analyze desorption data[5], are shown to have a complex dependence on the temporal moments.

Two modes of experimentation are possible for single-temperature desorption, in principle. In one the temperature of the adsorbent is instantaneously raised (as a step function) at time zero to a new contant value while flow of carrier gas is continuous. In the other mode the temperature is unchanged and flow is not begun until $t = 0$. In either case desorption is not observed until $t \geqslant 0$. The delay and spreading effects of inlet and exit lines attached to the reactor are easily established as additive contributions to the temporal moments.

Brenner and Hucul[4], who argued that isothermal desorption experiments avoid certain errors inherent in TPD experiments, proposed a method for analyzing the initial slope of a isothermal desorption response. The present theory relates the entire desorption peak to the transport model and its associated parameters.

THEORY

The method of analysis in this paper is to solve the governing equations for the desorption system in the Laplace domain, and then to derive temporal moment expressions by means of the relation

$$m_k = \int_0^\infty t^k c \, dt = \lim_{s \to 0} (-1)^k \frac{d^k c}{ds^k} \tag{1}$$

which follows directly from the definition of the Laplace transform. The normalized or reduced moments are given by

$$\mu_k' = m_k/m_0 \tag{2}$$

and the central moments by

$$\mu_k = \sum_{i=0}^{k} \binom{k}{i} (-\mu_1')^i \mu_{k-i} = \frac{1}{m_0} \int_0^\infty (t - \mu_1')^k c \, dt \tag{3}$$

It is well known that very complicated systems with interactions between kinetics and mass transfer can be analyzed in this manner as long as the differential equations and boundary conditions are linear[6,7].

The principal assumptions of the following analysis are:

(1) Species concentration is small enough that adsorption sites are unlimited, and initial adsorbed species concentration is uniform;

(2) Isotherms are linear;

(3) Adsorption and desorption rate expressions are linear;

(4) System temperature is uniform (no temperature gradients);

(5) Radial concentration gradients for the column are negligible;

(6) Porous particles are spherical (radius R) and homogeneous.

The governing differential equations for the CST model (with perfect mixing) when intraparticle diffusion is negligible is

$$\partial c/\partial t = -c/\tau - \left(\frac{1-\varepsilon}{\varepsilon}\right) \varrho_p \, \partial c_a/\partial t \tag{4}$$

where τ is the holding time of the packed bed. The initial conditions are

$$c(0) = c_0 \tag{5}$$

$$c_a(0) = c_{a0} = K_0' c_0 \tag{6}$$

For the column model we have

$$\varepsilon \partial c/\partial t + v \, \partial c/\partial z = D_\alpha \partial^2 c/\partial z^2 - (1-\varepsilon) \, \varrho_p \, \partial c_a/\partial t \tag{7}$$

with initial and boundary conditions,

$$c(0,z) = c_0 \tag{8}$$

$$c_a(0,z) = c_{a0} = K_0' c_0 \tag{9}$$

$$c(t,0) = 0 \tag{10}$$

$$c(t,\infty) = \text{finite} \tag{11}$$

In both cases the rates of adsorption and desorption are so fast that equilibrium is assumed:

$$c_a = K' c \tag{12}$$

In terms of dimensionless variables the moments for the CST model are

$$m_0^* = \varepsilon z^* (1 + \alpha K_0) \tag{13}$$

$$\mu_1'^* = \varepsilon z^* (1 + \alpha K) \tag{14}$$

$$\mu_2^* = \varepsilon^2 z^{*2} (1 + \alpha K)^2 \tag{15}$$

and for the column model,

$$m_0^* = \varepsilon z^* (1 + \alpha K_0) \tag{16}$$

$$\mu_1'^* = \frac{\varepsilon}{2} (z^* + 2/Pe)(1 + \alpha K) \tag{17}$$

$$\mu_2^* = \frac{\varepsilon^2 z^*}{12} (z^* + 12/Pe + 36/z^* Pe^2)(1 + \alpha K)^2 \tag{18}$$

The steady state approximation, $\partial c/\partial t \sim 0$, will hold when $\dfrac{1-\varepsilon}{\varepsilon} \varrho_p K' \equiv \alpha K \gg$

1. That is, for the case of very large adsorption capacities, the desorption process will be well-represented with the steady state assumption used in most papers on TPD.

In the column model the factors of 1/2 and 1/12 in the first and second moments, respectively, are characteristic of rectangular (plug flow) peaks, while the lack of such factors in the CST expressions is characteristic of the exponentially decreasing output peak of a well-stirred vessel. These factors are the significant differences between the two models.

The governing equations for the CST with intraparticle mass transfer effects are as follows:

inside the vessel,

$$\partial c/\partial t = -c/\tau - \frac{3}{R}\frac{(1-\varepsilon)}{\varepsilon} k_p (c - c_i) \tag{19}$$

inside a particle,

$$\beta \frac{\partial c_i}{\partial t} = D_i \frac{1}{r^2}\frac{\partial}{\partial r}\left(r^2 \frac{\partial c_i}{\partial r}\right) - \varrho_p \frac{\partial c_a}{\partial t} \tag{20}$$

reversible adsorption,

$$\frac{\partial c_a}{\partial t} = k_a c_i - k_d c_a \tag{21}$$

The initial conditions are

$$c(t = 0) = c_0 \tag{22}$$

$$c_i(t = 0) = c_0 \tag{23}$$

$$c_a(t = 0) = c_{a0} = K_0' c_0 \tag{24}$$

and boundary conditions are

$$c_i(r = 0) = \text{finite} \tag{25}$$

$$D_i \frac{\partial c_i}{\partial r}\bigg|_{r = R} = k_p (c - c_i) \tag{26}$$

The governing equations for the column model (6) are

$$\varepsilon \frac{\partial c}{\partial t} + v \frac{\partial c}{\partial z} = D_z \frac{\partial^2 c}{\partial z^2} - \frac{3}{R}(1 - \varepsilon) k_p (c - c_i) \tag{27}$$

Eqns. 20–24, for c_i, c_a, and for initial conditions are the same as for the CST model. In addition to the boundary conditions, eqns. 25 and 26, we have

$$c(t,0) = 0 \tag{28}$$

$$c(\infty,t) = \text{finite} \tag{29}$$

The moments for the CST model with intraparticle effects are

zeroth moment, $$m_0^* = \varepsilon z^*[1 + \alpha(\beta + K_0)] \tag{30}$$

first moment, $$\mu_1'^* = \Lambda_0 + \varepsilon z^*[1 + \alpha(\beta + K)] \tag{31}$$

where

$$\Lambda_0 = \alpha[\theta_d K_0 + (\beta + K_0)(\beta + K)(\theta_p/3 + \theta_D/15)]/[1 + \alpha(\beta + K_0)]$$

second moment, $$\mu_2^* = \Lambda_1 + 2(1 - \varepsilon)z^* \Lambda_2 + 2z^*\varepsilon[\alpha(\theta_d K + (\beta + K)^2 \times (\theta_p/3 + \theta_D/15)) + \varepsilon z^*(1 + \alpha(\beta + K))^2] - (\mu_1'^*) \tag{32}$$

where

$$\Lambda_1 = 2\alpha[\theta_d^2 K_0 + \theta_d K_0(\beta K/K_0 + \beta + 2K)(\theta_p/3 + \theta_D/15) +$$

$$\tfrac{2}{9}\theta_D(\beta + K_0)(\beta + K)^2(\theta_p/5 + \theta_D/35 + \theta_p^2/2\theta_D)]/[1 + \alpha(\beta + K_0)]$$

and

$$\Lambda_2 = [\theta_d K_0 + (\beta + K_0)(\beta + K)(\theta_p/3 + \theta_D/15)][1 + \alpha(\beta + K)]/[1 + \alpha(\beta + K_0)]$$

The moments for the column model with intraparticle diffusion are

$$m_0^* = \varepsilon z^*[1 + \alpha(\beta + K_0)] \tag{33}$$

$$\mu_1'^* = \Lambda_0 + \tfrac{1}{2}\varepsilon[1 + \alpha(\beta + K)](z^* + 2/Pe) \tag{34}$$

$$\mu_2^* = \Lambda_1 + (1 - \varepsilon)(z^* + 2/Pe)\Lambda_2 +$$

$$+ (1 - \varepsilon)(z^* + 2/Pe)[\theta_d K + (\beta + K)^2(\theta_p/3 + \theta_D/15)] +$$

$$+ \varepsilon^2 z^*(z^*/3 + 2/Pe + 4/z^*Pe^2)[1 + \alpha(\beta + K)]^2 - (\mu_1'^*)^2 \tag{35}$$

COMPARISON OF MODELS

All the models show that m_0^*, which is a measure of the total mass of solute eluted from the system, is independent of kinetic parameters and is a function only of the initial conditions, c_0, and $K_0 = c_{a0}/c_0$, as well as geometric parameters and velocity.

The dispersion appears as a "dispersive length", effectively increasing the length of the column. If in both column models the Peclet number, $Pe = vd/D_z$ becomes very large ($D_z \approx 0$), the dimensionless temporal moments for plug flow are obtained. More precisely, the requirement for plug flow is

$$z^* Pe \gg 1 \tag{36}$$

i.e. for sufficiently long columns dispersion effects may be neglected.

The first and second moments obviously show a complicated dependence on kinetic and mass transfer parameters. If the desorption rate, intraparticle diffusion, and mass transfer are negligible, the constraints for simplifying eqns. 30–35 are, respectively,

$$\theta_d \ll 1 \ (37), \ \theta_D \ll 1 \ (38), \text{and } \theta_p \ll 1 \quad (39)$$

The adsorption capacity will usually be very large compared to the intraparticle volume,

$$K \gg \beta \tag{40}$$

Under these conditions eqns. 13–18, for the cases of negligible intraparticle rate processes, are recovered from eqns. 30–35. The simplified equations will clearly be easier to use for calculations; thus efforts to satisfy experimentally the constraints 37–40 are rewarded with substantial reduction in computations for data analysis.

To compare the models we made some calculations for the desorption of propane from a column packed with porous silica gel[7]. Table I provides values of parameters and dimensionless groups[7]. The difference between column dispersion and plug flow models is small; the deviation from plug flow behavior for the first moment varies from 7 % for small reactor lengths ($z^* \approx 1$) to less than 1 % for $z^* = 30$. Similar deviations were found for the normalized second central moment. The conclusion is

TABLE I

PROCESS PARAMETERS[7] AND DIMENSIONLESS GROUPS FOR COMPARISON OF DESORPTION MODELS

Parameters		*Dimensionless groups*	
V	= 3.000 cm/sec	θ_d	= 0.956
ε	= 0.340	θ_p	= 0.020
R	= 0.050 cm	θ_D	= 6.284
ϱ_p	= 1.130 g/cm^3	Pe	= 18.600
β	= 0.486	K_0	= 71.190
D_z	= 0.125 cm^2/sec	K	= 71.190
D_i	= $1.540 \cdot 10^{-3}$ cm^2/sec		
k_p	= 9.620 cm/sec		
K'	= K_0 = 63.000 cm^3/g		
k_d	= 4.048 sec^{-1}		
d	= 0.775 cm		
c_0	= 1.000 moles/cm^3		

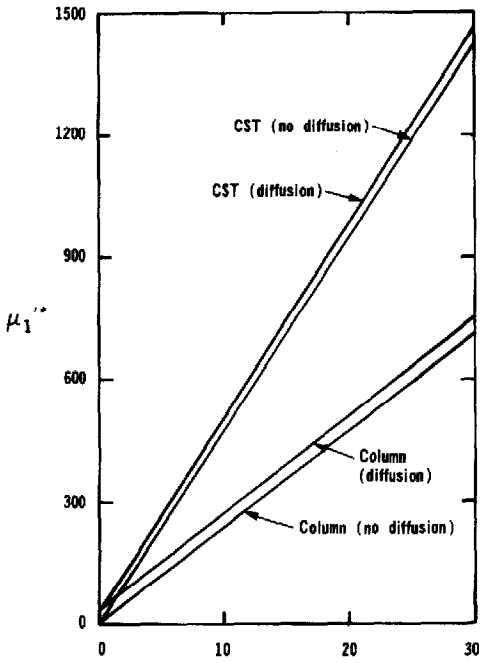

Fig. 1. Normalized first moment for desorption models.

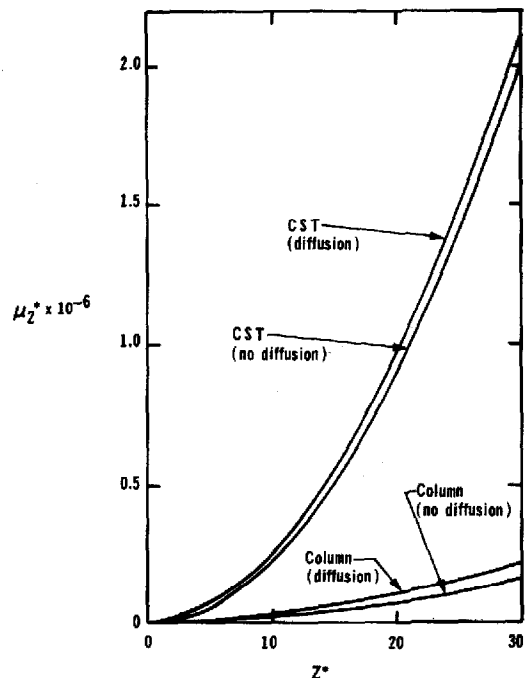

Fig. 2. Normalized second central moment for desorption models.

that longitudinal dispersion is a small but not necessarily negligible effect in column desorption.

The first and second moments for CST and column models with and without diffusion are plotted in Figs. 1 and 2. The models that include intraparticle diffusion allow for non-zero first and second moments for $z^* = 0$, in contradistinction to the simplified models. Thus for short columns diffusion and mass transfer effects may be noticeable, while for longer columns the relative magnitudes of the effects can be negligible.

The major differences between the CST and column models are the factors of 1/2 in the first moment and 1/12 in the second moment that appear for the column model and not in the results for the CST model (see eqns. 14, 15, 17 and 18). These substantial differences argue strongly against using a CST model to describe experiments in a column apparatus for large z^*. It will be noted from Figs. 1 and 2 that for $z^* = 1.45$ the curves for the CST model without diffusion cross those for the column model with diffusion for the particular values of parameters chosen.

PREDICTION OF ELUTION CURVES

Since it has not been possible to carry out the inverse Laplace transformation to find the analytical expression for the column diffusion model, we have chosen to use an expansion in orthogonal functions to represent the elution curve[8]. The Hermite polynomial expansion is a pertubation series for a Gaussian function, and is

chosen since it is well-known that when convection effects are more important than dispersion effects a typical chromatographic elution curve is nearly Gaussian. Corrections to the Gaussian shape would require that third and higher moments be known.

The expansion may be written[8],

$$c(z,t) = m_0 \, e^{-x^2} \sum_{n=0}^{\infty} a_n H_n(x) \tag{41}$$

where $x = (t - \mu_1')/\sqrt{2\mu_2}$. The Hermite polynomials are

$$H_0(x) = 1 \tag{43}$$

$$H_1(x) = 2x \tag{44}$$

$$H_2(x) = 4x^2 - 2 \tag{45}$$

$$H_3(x) = 8x^3 - 12x \tag{46}$$

$$\vdots$$

and have an orthogonality property that allows the expansion coefficients a_n to be evaluated,

$$a_0 = 1/\sqrt{2\pi\mu_2} \tag{47}$$

$$a_1 = a_2 = 0 \tag{48}$$

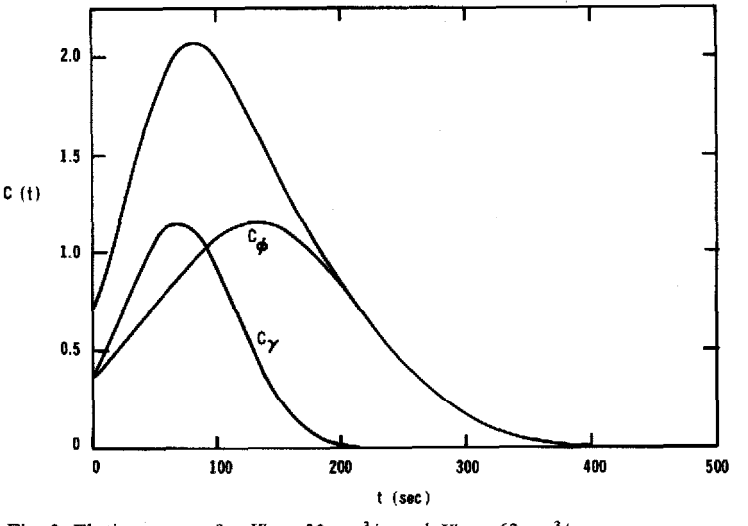

Fig. 3. Elution curves for $K_\gamma' = 33$ cm^3/g and $K_\phi' = 63$ cm^3/g.

$$a_3 = \mu_3/24\mu_2{}^2\sqrt{\pi} \tag{49}$$

$$\vdots$$

Because our purpose in this section is to study certain qualitative properties of elution curves, we need only the Gaussian approximation and hence only zeroth, first and second moments. The Gaussian approximation is given by

$$c(z,t) = \frac{m_0}{\sqrt{2\pi\mu_2}} \exp[-(t - \mu_1')^2/2\mu_2] \tag{50}$$

Given the case where an adsorbed species is held by two different sites, γ and φ, having different values of K and/or rate constants, concentration response will be the superposition of the two separate responses. In that case the total output concentration will be

$$c = c_\gamma + c_\varphi = \frac{m_{0\gamma}}{\sqrt{2\pi\mu_{2\gamma}}} \exp[-(t - \mu_{1\gamma}')^2/2\mu_{2\gamma}]$$

$$+ \frac{m_{0\varphi}}{\sqrt{2\pi\mu_{2\varphi}}} \exp[-(t - \mu_{1\varphi}')^2/2\mu_{2\varphi}] \tag{51}$$

We will assume the sites γ and φ differ only in values of K, *i.e.* $K_\gamma \neq K_\varphi$, since the effect of differing desorption rate coefficients is small. We use the parameter values of Table I with $z^* = 20$ and $c_0 = 1$ mol/cm^3. Figs. 3–5 show the elution curves for $K_\varphi = 33$ and $K_\gamma = 63$, 90, and 200 cm^3/g, respectively. The graphs show that for sufficiently different values of K, a bimodal peak will appear, while for smaller differences, overlapping of the appearance of a shoulder is observed. These results demonstrate that

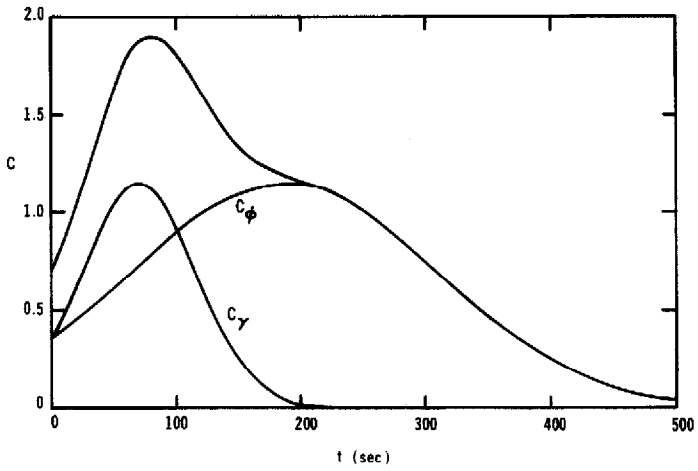

Fig. 4. Elution curves for $K_\gamma' = 33$ cm^3/g and $K_\varphi' = 90$ cm^3/g.

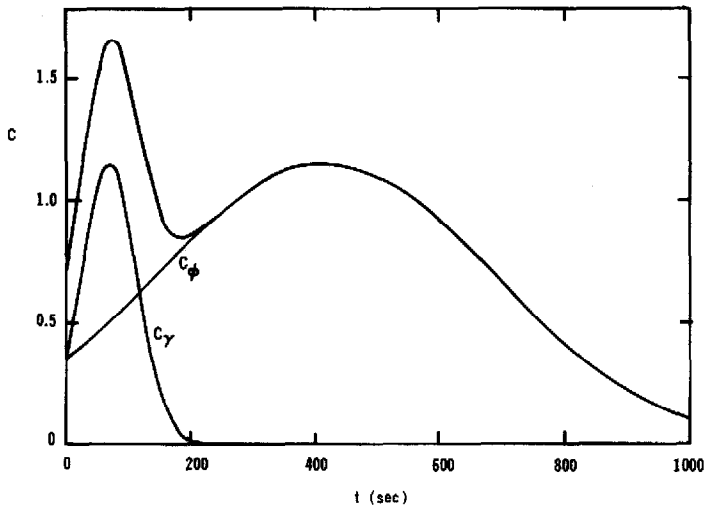

Fig. 5. Elution curves for $K'_\gamma = 33$ cm^3/g and $K'_\phi = 200$ cm^3/g.

bimodal behavior is not necessarily a result of temperature changes in TPD, but may also appear simply because of different equilibrium coefficients.

SHAPE INDICATORS AND TEMPORAL MOMENTS

The parameters previously used to describe the elution peaks of desorption experiments (either TPD or single-temperature desorption), and that can be determined from a single peak, have been defined as follows[5]:

(a) t_m = time for maximum concentration output;

(b) $\theta_m = \int_{t_m}^{\infty} c\,\mathrm{d}t$ = area under the concentration-time curve to the right of t_m;

(c) $\Delta t_{1/2}$ = peak width at half the maximum concentration;

(d) $S = (\mathrm{d}c/\mathrm{d}t)_{t_1}/(\mathrm{d}c/\mathrm{d}t)_{t_2}$ = shape index, where t_1 and t_2 are the inflection points of the concentration–time curve.

The relationship between these shape indicators and temporal moments will permit the prediction of shape indicators from moment expressions, given any desorption model.

We will approximate the concentration output as the expansion given by eqn. 41 up to the third-order terms:

$$c = m_0\, \mathrm{e}^{-\frac{(t-\mu'_1)^2}{2\mu_2}} \left[1/\sqrt{2\pi\mu_2} + \frac{\mu_3}{24\mu_2^2\sqrt{\pi}}\left(\frac{8(t-\mu'_1)^3}{\sqrt{8\mu_2^3}} - \frac{12(t-\mu'_1)}{\sqrt{2\mu_2}}\right)\right] \quad (52)$$

Setting the first derivative of eqn. 52 equal to zero will yield an equation for t_m,

$$\frac{\mu_3(t_m-\mu'_1)^4}{6\mu_2^3} - \frac{\mu_3(t_m-\mu'_1)^2}{\mu_2^2} + (t_m-\mu'_1) + \mu_3/2\mu_2 = 0 \quad (53)$$

The reader will notice that if $\mu_3 = 0$, then $t_m = \mu_1'$, so that the maximum concentration will coincide with the average time for a symmetrical peak. The maximum output concentration, c_{max} will be obtained by substituting t_m into eqn. 52.

Substituting eqn. 52 into the definition for θ_m, and performing the integrations, yields

$$\theta_m = \frac{m_0}{2}\left[\text{erfc}\left(\frac{t_m - \mu_1'}{\sqrt{2\mu_2}}\right) + \frac{\mu_3}{3\mu_2\sqrt{2\pi\mu_2}}\, e^{-\frac{(t_m - \mu_1')^2}{2\mu_2}}\left[\frac{(t_m - \mu_1')^2}{\mu_2} - 1\right]\right] \quad (54)$$

where erfc is the complementary error function. Note that if $\mu_3 = 0$, then $\theta_m = m_0/2$.

The quantity $\Delta t_{1/2}$ can be obtained from c_{max} divided by 2; then the difference of the two roots for $(t_{1/2} - \mu_1')$ that satisfy

$$\frac{(t_{1/2} - \mu_1')^2}{2\mu_2} = \ln\left[\frac{2m_0}{c_{max}\sqrt{2\pi\mu_2}}\left[1 + \frac{\mu 3(t_{1/2} - \mu_1')^3}{6\mu_2^3} - \mu_3\frac{(t_{1/2} - \mu_1')}{2\mu_2^2}\right]\right] \quad (55)$$

will give $\Delta t_{1/2}$. For a Gaussian peak ($\mu_3 = 0$), we find

$$t_{1/2} - \mu_1' = \pm\sqrt{1.386\mu_2} \quad (56)$$

so that

$$\Delta t_{1/2} = 2.355\sqrt{\mu_2} \quad (57)$$

The shape index, S, is determined from the time values that make zero the second derivative of the concentration function. That is, we need the roots of the fifth degree polynomial,

$$\frac{\mu_3(t - \mu_1')^5}{6\mu_2^4} - \frac{5\mu_3(t - \mu_1')^3}{3\mu_2^3} + \frac{(t - \mu_1')^2}{\mu_2} + \frac{5\mu_3(t - \mu_1')}{2\mu_2^2} - 1 = 0 \quad (58)$$

These roots are then substituted into the first derivatives of c to calculate S. This procedure clearly indicates that S depends on μ_1', μ_2, as well as μ_3. For a Gaussian curve, it is not difficult to show that $S \equiv 1$.

Because the temporal moments can be represented in terms of the transport and geometric parameters for a given CST or column model, the shape indicators can therefore have an extremely complicated dependence on the model parameters. Furthermore, since details are sensitive to experimental errors, caution is urged against uncritical use of shape indicators as diagnostics for desorption data.

CONCLUSIONS

An objective of this work has been to examine the models, assumptions, and procedures used to analyze thermal desorption processes for beds of porous particles. The analysis has been based on a constant temperature desorption process, while most experiments reported in the literature are temperature programmed. The major

conclusion of this work regarding mass transfer resistances, however, applies to either mode of operation, because the parameters describing mass transfer and diffusion do not vary strongly with temperature. Thus, the differences between column and CST models, and criteria for neglecting dispersion of intraparticle mass transfer effects, provided by the present analysis, should hold true for both constant and programmed temperature desorption.

A disadvantage of temperature programmed desorption as compared with single-temperature desorption (STD) is that because of the varying temperature, the temperature-dependent parameters, *e.g.* K, cannot be directly measured at a single temperature. For STD, on the other hand, equations for moments can be used, for example, to determine K. If ε, z^* and β are known, values of K may be calculated from first and second moments and compared to assess accuracy. Brenner and Hucul[4] have commented further on possible errors due to thermocouple response times that can be large in TPD.

Another approach that makes use of zeroth moment information, is to use eqn. 33 for m_0^* to determine K_0. Then, the first moment would yield K. A STD experiment at another temperature would provide K at that temperature. In this moment STD experiments at several tempertures could be utilized to establish the temperature dependence of K.

The theory presented in this work applies only to a first-order desorption rate process, which is valid for sufficiently dilute concentrations. The linearity can be tested by performing two STD experiments at the same temperature, but with different concentrations of solute. In the desorption expression is indeed linear within the concentration range, the increase in concentration will not alter the estimated value of K.

From the results obtained for column diffusion and CST-diffusion models, it is clearly seen that the zeroth moments (areas under the peaks) are independent of temperature of desorption, *i.e.*, independent of kinetic or rate parameters. They are functions only of the initial conditions or equilibrium constant K_0. It can also be seen that the zeroth moment expressions for these models are equivalent for the CST and column models without intraparticle diffusion and mass transfer considerations. This is necessarily true since the zeroth moments represent the total mass eluted from the system.

The first and second moments, which are proportional to the centroid of mass and to the width of an elution peak, respectively, depend on all factors characterizing the system, *i.e.*, geometrical features, equilibrium parameters, and transport properties. The first and second moments increase with increasing size of particles, equilibrium constant, and for the case of column-diffusion model with increasing dispersion coefficient. They decrease with increasing desorption, diffusion, and mass transport rates, and for the column-diffusion model with increasing fluid velocity.

From the comparison between models, it can be concluded that for the particular gas–solid desorption process used in the analysis, and more likely for the other common cases of gas–solid desorption process, the dispersion effect in the column models can be neglected for long columns or small axial dispersion ($z^* \gg 1/Pe$) without appreciable consequences. Desorption, mass transfer, and diffusion inside pores of solid support have noticeable effects, particularly in the normalized second central moment, for small reactor lengths. These effects become smaller as the length

of the reactor is increased. Depending on the reactor dimensions and desired accuracy, the intraparticle effects could be neglected. Nevertheless, important kinetic information can be obtained from the $\mu_1'^*$ values with mass transfer and diffusion considerations, since in a plot of $\mu_1'^*$ *versus* z^*, the intersection with the $\mu_1'^*$ axis will give a known function of k_d, k_p and D_i.

We have shown that the steady-state condition for the desorption models will hold when the system shows high adsorption capacity or very low desorption rate. Under these circumstances the concentration response will be characterized by high $\mu_1'^*$ and μ_2^* values, *i.e.*, by long retention times and wide output peaks. The implementation of the steady-state approximation when high adsorption capacities or small desorption rates are not present in the desorption system will result in shorter retention times and narrower concentration peaks than the ones characterizing the actual process.

Our results show that a constant temperature desorption will yield a peak whose shape can be described in terms of the moments via an expansion in orthogonal functions. The results obtained when two adsorption sites differing in equilibrium constant values were considered for the prediction of elution curves demonstrate that the bimodal behavior of concentration responses is not necessarily a result of temperature programmed desorption processes.

SYMBOLS

c = concentration (moles/vol)
c_a = concentration of adsorbed species (moles/mass of particle)
c_i = concentration in pores (moles/vol)
d = column diameter (length)
D_i = effective intraparticle diffusion coefficient (length^2/time)
D_z = axial dispersion coefficient (length^2/time)
k_a = adsorption rate coefficient (vol/mass time)
k_d = desorption rate coefficient (1/time)
k_p = particle mass transfer coefficient (length/time)
K' = equilibrium coefficient (vol/particle mass)
m_k = kth temporal moment (moles time $^{k+1}$/vol)
r = particle radial coordinate (length)
R = radius of particle (length)
t = time
v = superficial velocity = flow-rate/column cross-section (length/time)
z = column length co-ordinate (length)
α = $(1 - \varepsilon)/\varepsilon$
β = particle porosity
ϱ_p = particle density (mass/vol)
μ_1' = normalized first temporal moment (time)
μ_2' = normalized second central moment (time^2)
ε = reactor void fraction
τ = reactor holding time (time)

Dimensionless groups

$K = \varrho_p K'$

$m_k^* = m_k v^{k+1}/c_0 d^{k+1}$

$Pe = vd/D_z$

$z^* = z/d$

$\mu_1'^* = \mu_1' v_0/d$

$\mu_2^* = \mu_2 v^2/d^2$

$\mu_2 v^2/d^2$

$\theta_d = v_0/dk_d$

$\theta_D = R^2 v/dD_i$

$$\theta = \int_{t_m}^{\infty} c\,dt$$

$\theta_p = Rv/dk_p$

Subscripts

0 = initial condition

k = 0, 1, 2, ...

REFERENCES

1 M. Smutek, S. Cerny and F. Buzek, *Advan. Catal.*, 24 (1975) 343.
2 R. J. Cvetanovic and Y. Amenomiya, *Advan. Catal.*, 17 (1967) 144.
3 V. R. Choudhary, *J. Chromatogr.*, 157 (1978) 391.
4 A. Brenner and D. A. Hucul, *J. Catal.*, 46 (1979) 134.
5 E. E. Ibok and D. F. Ollis, *J. Catal.*, 66 (1980) 391.
6 T. Furusawa, M. Suzuki and J. M. Smith, *Catal. Rev. —Sci. Eng.*, 13 (1976) 43.
7 P. Schneider and J. M. Smith, *AICh J.*, 14 (1968) 762.
8 R. V. Mehta, R. L. Merson and B. J. McCoy, *J. Chromatogr.*, 88 (1974) 1.